www.serd.ait.ac.th/reric

An Improved Method for Dynamic Voltage Collapse Prediction in Power System (September 2006)

Muhammad Nizam, Azah Mohamed and Aini Hussain

Abstract *- This paper presents an improved method for predicting dynamic voltage collapse in power systems by developing the power transfer stability index. The generator governor and excitation dynamics, induction motor and under load tap changer are considered in the simulation process. Time domain simulations using the PSAT software program has been carried out in this work. Several contingencies have also been considered in the simulations including real and reactive power load increase, line outage and generator outage. The proposed PTSI index has been investigated for its applicability in indicating proximity to voltage collapse. The performance of the index was tested using the thirty nine-bus test system and studied under various operating conditions. Simulation test results prove that the proposed PTSI index gives a better prediction of dynamic voltage collapse compared to the voltage collapse prediction index.*

Keywords **- Dynamics, voltage collapse, time domain simulation, voltage stability**

1. INTRODUCTION

Voltage instability problem has been a serious limitation in power system operation in which a large number of blackouts are due to this form of instability. As system load increases, voltage magnitudes throughout a power network will slowly decline and continuing increase in loads may eventually drive a power system to a state of voltage instability and may cause a voltage collapse. Recent blackouts around the world are mainly due to voltage collapse occurring in stressed power systems which are associated with low voltage profiles, heavy reactive power flows, inadequate reactive support and loads. The consequences of voltage collapse are that system restoration takes a long time with large groups of customers left without supply for extended period of time. The study of voltage instability and voltage collapse is therefore still a major concern in power system operation and planning.

Several different approaches have been proposed for predicting the occurrence of voltage collapse. Most of the works addressed in the literature treat voltage instability problem using static analysis methods based on the conventional power flow model. The static analysis of voltage instability produces some results but it does not take into account of the dynamic aspects of power systems. An electrical power system is typically a large dynamic system in which the dynamic behavior of its components has a significant influence on voltage collapse. Governor and exciter of a generator and induction motor load could affect voltage stability [1]. To incorporate the dynamic aspects of a power system into voltage stability analysis, accurate modeling of power system components is required and time domain simulation is normally implemented. Another important aspect in dynamic voltage stability analysis is the impact of contingencies on power system operation. The contingencies normally considered are load increase, line outage and generator outage.

In predicting dynamic voltage collapse, many indices are used to determine how far a power system is from voltage collapse. Several research works have been carried out focusing on how to accurately estimate the dynamic voltage stability margin and to predict the occurrence of dynamic voltage collapse [14].

Some of the well known methods for predicting proximity to dynamic voltage collapse use eigenvalue analysis [2-4] and voltage stability indices such as the power margin [5-6], line index [7] and voltage collapse prediction index [8]. Ref. 15 determines the voltage stability margin of a power system by using information about the current operating point. The method simply requires some locally measurable quantities, such as bus voltage magnitude and active and reactive components of load power. In this paper, an improved method for dynamic voltage collapse prediction using the power transfer stability index (PTSI) is proposed and presented. This index is based on the ratio of the apparent load power to the maximum load power transfer at particular bus. In the dynamic simulation of voltage collapse, power system dynamic models have been incorporated including induction motor, generator excitation limiter, automatic voltage regulator and under load tap changer (ULTC). Some generic load models are also considered [16]. The 39-bus test system is used for carrying out the simulation of dynamic voltage

M. Nizam has been working at the Engineering Department, Sebelas Maret University, Indonesia. He is currently a Ph.D Student at the Department of Electrical, Electronic and Systems Engineering, Universiti Kebangsaan Malaysia, Bangi 43600, Selangor, Malaysia, Majoring in Power System (corresponding author, Phone : 60-3-89216590, e-mail: nizam_kh@vlsi.eng.ukm.my).

A. Mohamed is a Professor at Department of Electrical, Electronic and System Engineering, Universiti Kebangsaan Malaysia, specializing in voltage stability studies, (email : azah@vlsi.eng.ukm.my).

A. Hussain is an Associate Professor at the Department of Electrical, Electronic and Systems Engineering, Universiti Kebangsaan Malaysia, specializing in Signal Processing, (email: aini@vlsi.eng.ukm.my).

collapse. The time domain simulations are carried out using the Power System Analysis Toolbox (PSAT) simulation program [9].

2. INDICES FOR DYNAMIC VOLTAGE COLLAPSE PREDICTION

The derivation of the power transfer stability index (PTSI) is presented in this section. Another index named as the voltage collapse prediction index VCPI [8] is also described because this index is used for the purpose of comparing with the proposed index.

Derivation of the Power Transfer Stability Index

The proposed power transfer stability index (PTSI) is derived by first considering a simple two-bus Thevenin equivalent system, where one of the buses is a slack bus connected to a load bus by a single branch as shown in Fig. 1. Referring to Fig. 1, the current drawn by the load is given by,

$$\bar{I} = \frac{\bar{E}_{Thev}}{\bar{Z}_{Thev} + \bar{Z}_L} \tag{1}$$

The load apparent power can be written as,

$$\bar{S}_L = \bar{Z}_L \bar{I}\ \bar{I}^* = \bar{Z}_L \left|\bar{I}\right|^2 \tag{2}$$

Substituting (1) into (2) yields,

$$\bar{S}_L = \bar{Z}_L \left| \frac{\bar{E}_{Thev}}{\bar{Z}_{Thev} + \bar{Z}_L} \right|^2 \tag{3}$$

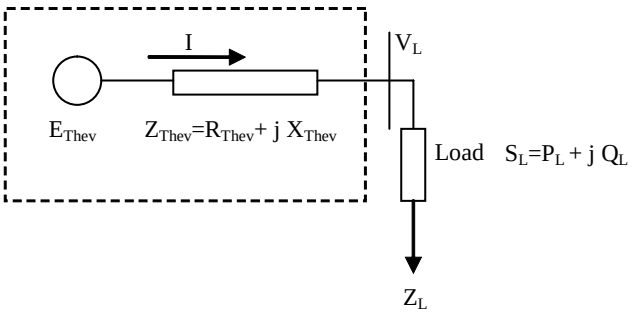

Fig. 1. Simple two-bus thevenin equivalent system.

Considering $\bar{Z}_L = Z_L \angle \alpha$ and $\bar{Z}_{Thev} = Z_{Thev} \angle \beta$ and substituting both into (3), we get,

$$\bar{S}_L = Z_L \angle \alpha \left| \frac{E_{Thev}}{Z_{Thev}\ \angle \beta + Z_L\ \angle \alpha} \right|^2 \tag{4}$$

where α is phase angle of the load impedance and â is phase angle of the Thevenin impedance.

The magnitude of load apparent power S_L from (4) can be expressed as,

$$S_L = \frac{E_{Thev}^2 Z_L}{\left| Z_{Thev} \angle \beta + Z_L \angle \alpha \right|^2} \tag{5}$$

Simplifying (5), we get

$$S_L = \frac{E_{Thev}^2 Z_L}{Z_{Thev}^2 + Z_L^{\ 2} + 2 Z_{Thev} Z_L \cos(\beta - \alpha)} \tag{6}$$

To determine the maximum load apparent power S_L, the condition of $\partial S_L / \partial Z_L$ must be met. By differentiating (6) with respect to the load impedance Z_L and by determining maximum value of S_L in which $\partial S_L / \partial Z_L = 0$, hence,

$$\frac{\partial S_L}{\partial Z_L} = \frac{E_{Thev}^2 \left(Z_{Thev}^2 - Z_L^2 \right)}{\left[Z_{Thev}^2 + Z_L^2 + 2 Z_{Thev} Z_{L0} \cos(\beta - \alpha) \right]^2} = 0 \tag{7}$$

From (7), the point of maximum loadability can be determined when $Z_{Thev}^2 - Z_L^2 = 0$ or $Z_L = Z_{Thev}$

The maximum load apparent power S_{Lmax} is then determined by substituting $Z_L = Z_{Thev}$ into (6) and simplifying it further, we get,

$$S_{L\max} = \frac{E_{Thev}^2}{2 Z_{Thev} (1 + 2\cos(\beta - \alpha))} \tag{8}$$

The maximum load apparent power given by (8) is also considered as the maximum loadability limit which depends on the Thevenin parameters that vary with system operating conditions.

To assess the load bus distance to voltage collapse, a power margin is defined as $(S_{Lmax} - S_L)$ in which the margin is equal to 0 if $Z_L = Z_{Thev}$. For power margin values equal to 0, it indicates that no more power can be transferred at this point and a proximity to voltage collapse is said to occur. Thus, to prevent a power system from voltage collapse, the power margin has to be greater than zero. In other words, the ratio of S_L to S_{Lmax} has to be less than 1.0. However, a voltage collapse will occur if the ratio of S_L to S_{Lmax} is equal to 1, that is,

$$\frac{S_L}{S_{L\max}} = 1 \tag{9}$$

Substituting (6) and (8) into (9), we get

$$\left[\frac{E_{Thev}^2 Z_L}{Z_{Thev}^2 + Z_L^{\ 2} + 2 Z_{Thev} Z_L \cos(\beta - \alpha)} \right] \left[\frac{2 Z_{Thev} (1 + \cos(\beta - \alpha))}{E_{Thev}^2} \right] = 1 \tag{10}$$

Simplifying (11), we get,

$$\frac{2S_L Z_{Thev}(1+\cos(\beta-\alpha))}{E_{Thev}^2}=1 \quad (11)$$

Using (12), the proposed voltage collapse index, PTSI becomes

$$PTSI=\frac{2S_L Z_{Thev}(1+\cos(\beta-\alpha))}{E_{Thev}^2} \quad (12)$$

The values of PTSI will fall between 0 and 1. When PTSI value reaches 1, it indicates that a voltage collapse has occurred.

Formulation of the Voltage Collapse Prediction Index

The calculation of the voltage collapse prediction index (VCPI) requires voltage phasor information of the participating buses in a system and network admittance matrix. The VCPI [8] for bus k can be written as,

$$VCPI_k=1-\frac{\sum_{\substack{m=1\\ m\neq k}}^{N} V'_m}{V_k} \quad (13)$$

In which V'_m is given by,

$$V'_m=\frac{Y_{km}}{\sum_{\substack{j=1\\ j\neq k}}^{N} Y_{kj}}V_m \quad (14)$$

where,

V_k is the voltage phasor at bus k
V_m is the voltage phasor at bus m
Y_{km} is the admittance between bus k and m
Y_{kj} is the admittance between bus k and j
k is the monitoring bus
m is the other bus connected to bus k

The value of VCPI varies between 0 and 1. If the index is zero, the voltage at bus k is considered stable and if the index is unity, a voltage collapse is said to occur.

Procedure for Simulation of Dynamic Voltage Collapse

The dynamic simulation of voltage collapse study was carried out using the Power System Analysis Toolbox (PSAT) software program [9]. The procedures in simulating dynamic voltage collapse are described as follows:

i. Input load, generator and line data of the test system.
ii. Create seven cases of contingency conditions such as step increase in load, line outage, generator outage and effect of ULTC.
iii. Run the time domain simulation for 200 seconds or until the simulation stops when the Jacobian matrix becomes singular.
iv. At every time step of 1 second, measure the voltage, phase angle, real power and reactive power at all monitoring buses.
v. Using the data obtained from step (iv), calculate the Thevenin voltage, E_{thev}. and Thevenin impedance, Z_{thev} at every load bus in every second. The Thevenin voltage and Thevenin impedance are required for the calculation of the indices PTSI and VCPI. The procedure to calculate E_{thev} and Z_{thev} is explained and given as in the Appendix.
vi. Calculate the PTSI and VCPI indices at every time step of 1 second.
vii. Plot the indices against time.
viii. Repeat steps (ii) to (vii) by considering another case of operating condition.

All simulations use a time sampling of one second in which at this sampling time the transient effect is not noticeable.

3. TEST SYSTEM DESCRIPTION

The 39 bus test system which is used in the dynamic simulation is shown in Fig. 2 in which it consists of ten generators connected at buses 30 to 39 and bus 31 is the slack bus.

All generators are equipped with identical automatic voltage regulator (AVR), over excitation limiters (OEL) and turbine governor. The bus and line data of the test system can be found in Ref. 17.

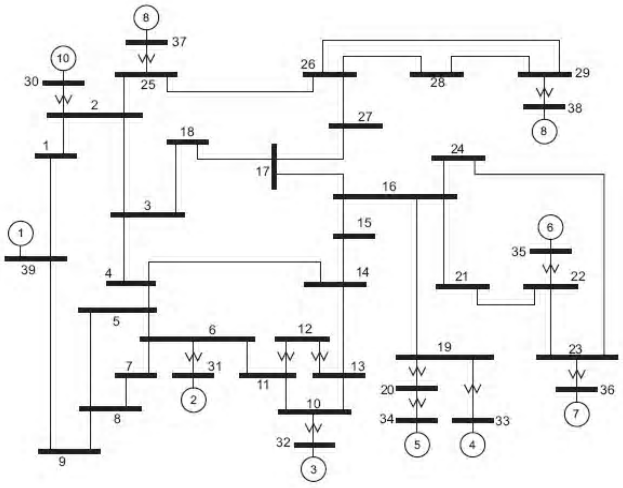

Fig. 2. One-line diagram of the 39-bus test system.

Generator and Load Modeling

All the ten generators have identical dynamic characteristics using the sixth order synchronous machine model (two axes, with two windings on each axis) for each generator [9]. The AVR of IEEE model 1 and the type 1 steam turbine governors as shown in Figs. 3(a) and 3(b) are used in the study. Both AVR and over excitation limiter (OEL) regulate the voltage at the generator terminal by performing both regulating and excitation system stabilizing functions. The AVR defines the primary voltage regulation of the generator while the OEL provides an additional signal to the reference voltage of AVR [12]. The detailed parameters of the AVR and OEL are as shown in Tables 1 and 2, respectively. The turbine governor of Type 1 [9] defines the primary frequency regulation of the synchronous generators in which the turbine governor parameters are given in Table 3.

For dynamic loads, the model considered is the voltage dependent load with active and reactive power voltage dependence of $\alpha = 1.8$ and $\beta = 0.5$, respectively. As for the static loads, constant PQ load model is considered in which the load data can be found in Ref. 17.

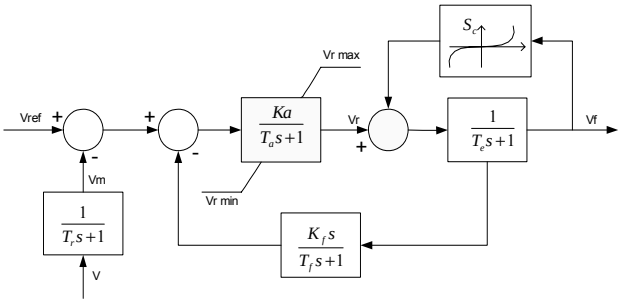

Fig. 3a. AVR – IEEE model 1.

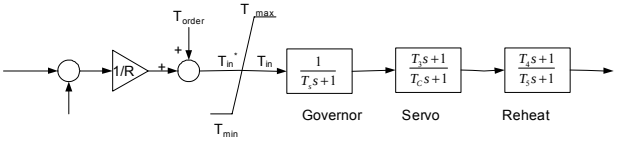

Fig. 3b. Turbine governor – type 1.

The system also considers six induction motors which have identical dynamic characteristics. The type of induction motor used is the single cage induction motor model. These motors are connected at bus 4, 12, 16, 21 and 23 with ratings of 500 + j184 MVA, 8.5 + j88 MVA, 329 + j32.3 MVA, 274 + j115 MVA, and 247.5 + j84.6 MVA, respectively. The detailed specification of each induction motor can be found in Ref. 11 with stator resistance (R_s) = 0.01 p.u., stator reactance (X_s) = 0.15 p.u., rotor resistance (R_R) = 0.05 p.u., rotor reactance (X_R) = 0.15 p.u., magnetization reactance (X_m) = 5 p.u. and inertia constant (H) = 3 KWs/KVA.

ULTC Transformer Modeling

The ULTC is used for controlling the secondary voltage [13]. Its action is represented with time delay and deadband in which the time delay for ULTC is assumed to be 1 second. The tap ratio considered has a minimum and maximum voltage tap of 0.8 p.u. and 1.2 p.u., respectively, with a step of 0.025 p.u. per tap or 16 steps.

Table 1. AVR System Parameter – Type IEEE Model 1

Stabilizer gain K_f	Stabilizer Time Constant T_F	Amplifier gain K_A	Amplifier Time Constant T_A	Field Time Constant T_e	Measurement Time Constant T_r	Max Regulator Output V_{RMAX}	Min Regulator Output V_{RMIN}
0.03	1.0 sec	5	0.02 sec	0.8 sec	0.001 sec	5 pu	-5 pu

Table 2. Specification of Over Exciter Limiter

Integrator Time Constant T_0	d-axis estimated generator reactance x_d	q-axis estimated generator reactance x_q	Maximum field current I_{flim}
0.03 sec	0.2 pu	0.18 pu	1.0 pu

Table 3. Specification of Turbine Governor – Type 1

Reference Speed ω_{Ref}	Droop R	Max Turbin Output T_{max}	Min Turbin Output T_{min}	Governor Time Constant T_S	Servo Time Constant T_C	Transient Gain Time Constant T_3	Power Fraction Time Constant T_4	Reheat Time Constant T_5
1 p.u.	0.05	16 p.u.	0.75 p.u.	0.1 sec	0.45 sec	0 sec	12 sec	50 sec

Table 4. Simulation Test Cases

Test Case	Contingency	System Load	Control measures
A	Increase P and Q loads at bus 15 at a rate of 0.1 + j0.05 p.u.-MVA/sec with initial load of 3.20 + j1.53 p. u.	Static loads	AVR, OEL
B	Increase P and Q loads at bus 15 at a rate of 0.1 + j0.05 p.u.-MVA/sec with initial load of 3.20+j1.53 p. u.	Induction motors	AVR, OEL
C	Increase P load at bus 15 at a rate of 0.1065 p.u.-MW/sec with initial load of 3.20 + j1.53 p. u.	Induction motor and static loads	AVR, OEL
D	Increase Q load at bus 15 at a rate of 0.1065 p.u.-MVAR/sec with initial load of 3.20 + j1.53 p. u.	Induction motor and static loads	AVR, OEL
E	Multiple Line Outages at line 14-15, and 13-14. Increase P and Q loads at bus 15 at a rate of 0.1 + j0.05 pu/s with initial load of 3.20+j1.53 p.u.	Induction motor and static loads	AVR, OEL
F	Outage of Generator at bus 30. Increase P and Q loads at bus 15 at a rate of 0.1 + j0.05 p.u./sec with initial load of 3.20 + j1.53 p. u.		AVR, OEL
G	Increase P and Q loads at bus 15 at a rate of 0.1 + j0.05 p.u./sec with initial load of 3.20 + j1.53 p. u.	Induction motor and static loads.	AVR,OEL,ULTC connected at lines 14-15 and 13-14

4. TEST RESULTS

In this study, seven test cases have been considered as described in Table 4. Simulations were carried out to evaluate the performance of the proposed PTSI indicator in predicting dynamic voltage collapse as well as to examine the behavior of excitation system, ULTC and induction motor load during voltage instability condition.

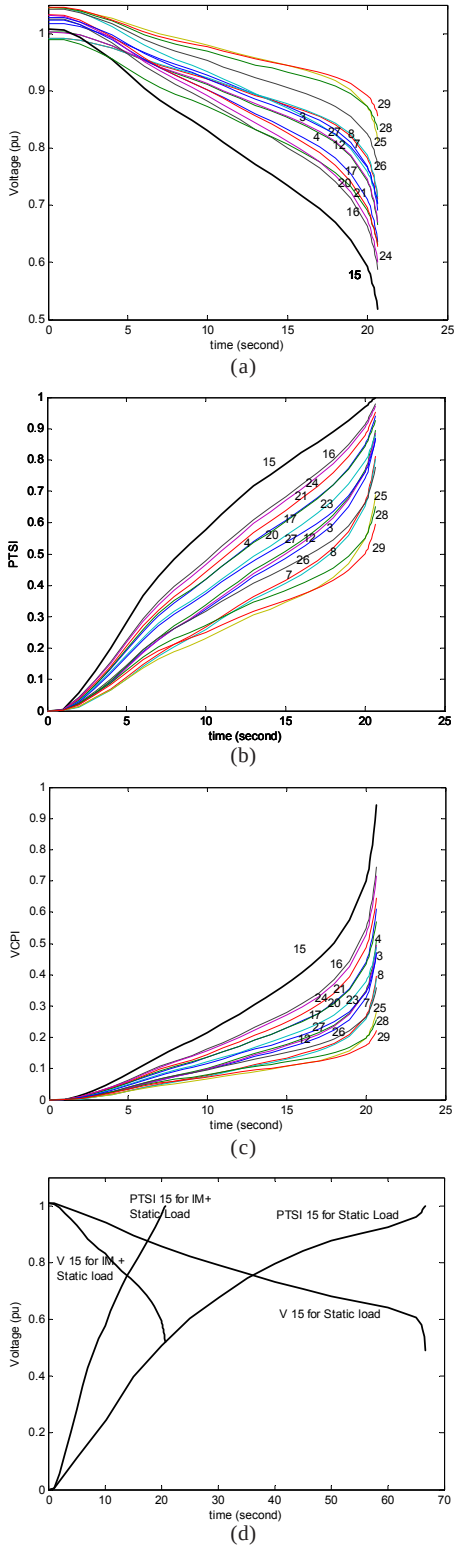

Fig. 4. Effect of induction motor a) Voltage vs time at several load buses b) PTSI vs time at several load buses c) VCPI vs time at several load buses d) Comparing the effect of different types of loads on voltage collapse.

Behavior of Induction Motor Load during Dynamic Voltage Collapse

Simulations were carried out for test cases A and B so as to compare the behavior of induction motor and static loads and to investigate the effect of induction motor loads in the dynamic simulation of voltage collapse. In test case A, static loads are connected at 18 load buses of bus 3, 4, 7, 8, 12, 15, 16, 17, 20, 21, 23 to 29 and 39 while in test case B, dynamic loads which are voltage dependent loads are connected at 13 load buses of bus 3, 7, 8, 15, 17, 20, 24 to 29 and 39 with five induction motor loads connected at bus 4, 12, 16, 21 and 23. To simulate a voltage collapse condition in both test cases A and B, a step increase in load is considered in which the static load at bus 15 is increased at a rate of 0.1 + j0.05 p.u. (MVA/sec) from an initial load of 3.20 + j1.53 p.u. MVA. In the simulation for test case B, the bus voltages at all the load buses are recorded and plotted against time as shown in Fig. 4(a). The figure shows that bus 15 has the lowest voltage bus and the highest rate of voltage with respect to load changes.

The voltage stability indices PTSI and VCPI measured at all the load buses are plotted against time as shown in Figs. 4(b) and 4(c), respectively. From the figures, it can be seen that the values of PTSI and VCPI indices increase as the load at bus 15 is increased. It is also noted that bus 15 is more prone to voltage collapse as compared to the other buses because highest values of PTSI and VCPI indices are recorded at bus 15 in which the values of PTSI and VCPI indices at bus 15 are 0.999 and 0.983, respectively.

To investigate the effect of different types of loads on dynamic voltage collapse, simulations were carried out for the case of system with static loads only as in test case A and for system with both static and induction motor loads as in test case B. The results for both test cases are as shown in Fig. 4(d). From the figure, it can be seen that system with induction motor loads collapses faster at t = 20.5 sec when PTSI at bus 15 indicates a value of 0.999 as compared to the system with static loads only in which voltage collapse occurs at t = 76 sec when the PTSI value at bus 15 is 0.998. The results prove that the system with induction motors give more effect to voltage collapse compared to system with only static loads because the motors absorb much more reactive power thus causing the voltage to drop faster than static loads [6].

Effect of Increasing Either Real or Reactive Power Loads

Test cases C and D are considered to investigate the effect of increasing either real or reactive loads in the dynamic simulation of voltage collapse. For both test cases, an initial load of 3.20 + j1.53 p.u. is considered at bus 15. However, in test case C, the static load at bus 15 is increased at a rate of 0.106 p.u. (MW)/sec of real power whereas in test case D, the static load at bus 15 is increased at a rate of 0.106 p.u. (MVar) /sec of reactive power. The simulation results of test cases C and D are plotted in Figs. 5 and 6, respectively. From the figures, it can be seen that the PTSI and VCPI indices increase with time as loads are increased at bus 15

and the point of collapse (PoC) occurs when both the values of PTSI and VCPI approach 1.0. Comparing the effect of increasing either real and reactive power loads, it is noted that the system collapses faster when reactive power is increased in which voltage collapse occurs at time t = 18.25 sec as compared to time t = 21.3 sec for pure real load increase. Fig. 7 illustrates further the effect of increasing different types of loads at bus 15. The figure shows that the increase in pure reactive load gives more significant effect to voltage collapse at bus 15 than increase in real power load or mixed real and reactive power load.

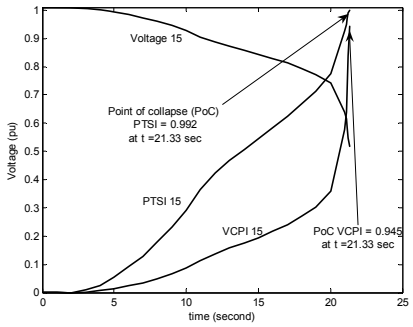

Fig. 5. PTSI and VCPI indices due to increase in real power load.

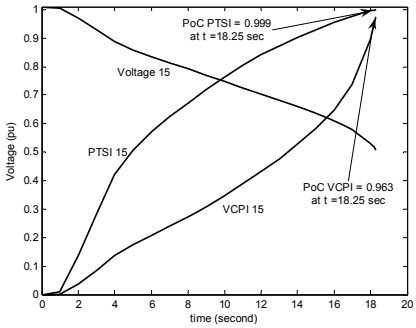

Fig. 6. PTSI and VCPI indices due to increase in reactive power load.

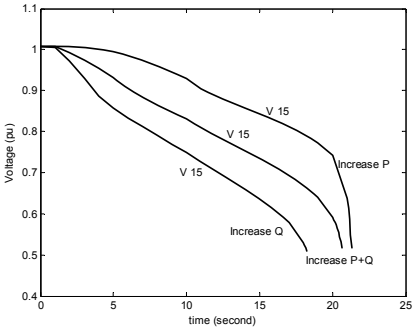

Fig.7. Voltage at bus 15 for comparing the effect of increasing real and reactive power loads.

Voltage Collapse due to Multiple Line Outages

Test case E is considered to investigate the effect of multiple line outages in the dynamic simulation of voltage collapse. In this test case, the system has induction motors connected at the five buses similar to that in test case B and two lines connecting buses 13-14 and 14-15 are outaged or disconnected at time t = 2 secs. The results of the PTSI and VCPI indices of bus 15 are plotted against time as shown in Figs. 8(a) and 8(b), respectively.

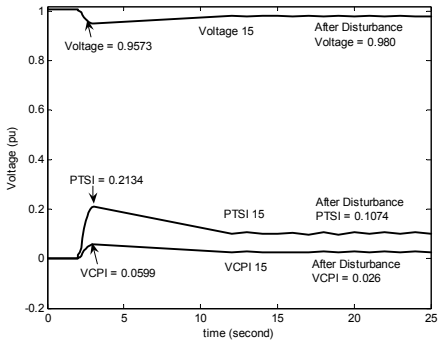

a) PTSI and VCPI indices due to lines outage without load increase.

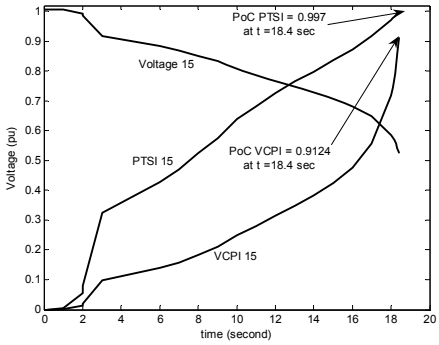

b) PTSI and VCPI indices due to lines outages with load increase.

Fig. 8. Effect of lines outage.

Figure 8(a) shows that the both the PTSI and VCPI values are low, that is, very much less than 0.3 and that the voltage at bus 15 does not seem to collapse. The results indicate that the multiple line outages of lines connecting buses 13-14 and 14-15 without any load increase at bus 15 do not cause voltage instability in the system. However, by simulating both line outages 13-14 and 14-15 and gradual load increase at bus 15, the system will collapse as shown in figure 8b in which the point of collapse occurs at time t = 18.4 sec when the values of PTSI and VCPI are 0.997 and 0.9124, respectively. In this case, the lines 13-14 and 14-15 are vital lines serving load bus 15 and outage of these line will create adverse effect on bus 15. Additional load increase at bus 15 will cause a voltage collapse in the system.

Voltage Collapse due to Generator Outage

Test case F is to investigate the effect of generator outage in the dynamic simulation of voltage collapse. In the simulation, the static load at bus 15 is increased at a rate of 0.1 + j0.05 p.u./sec from initial load of 3.20 + j1.53 p.u. and the generator at bus 30 is outaged. The PTSI and VCPI indices of load bus 15 are plotted against time for this contingency case as shown in figures 9a and 9b. Figure 9a shows that the effect of a generator outage at bus 30 does not create voltage instability in the system. However, by

simulating both a generator outage at bus 30 and a gradual load increase at bus 15, a voltage collapse is said to occur at time t = 18.5 sec when both the PTSI and VCPI values reach 0.998 and 0.959, respectively.

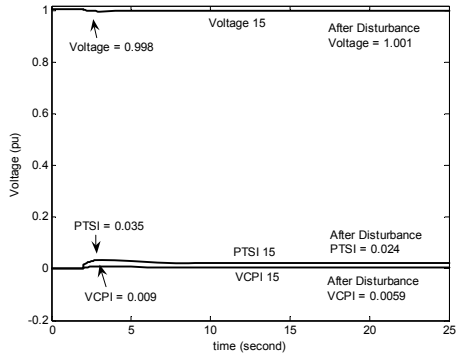

a) PTSI and VCPI indices due to generator outage without load increase.

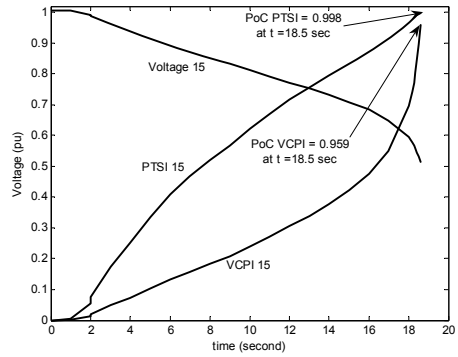

b) PTSI and VCPI indices due to generator outage with load increase.

Fig. 9. Effect of generator outage.

Effect of Installing ULTC Transformer

Test case G is considered to investigate the effect of installing two ULTCs at lines connecting buses 13-14 and 14-15. A similar operating condition as in test case B is simulated but in this case, the ULTCs are installed. Figure 10 shows the effect of installing ULTCs in the system in which the result shows that voltage collapse occurs later than for the case without ULTCs. It can be seen from the figure that by installing ULTCs, the time of collapse at bus 15 is extended by 6 %. Thus, the use of ULTC transformers help to boost up voltage magnitudes of the installed load buses and improve voltage stability of the system.

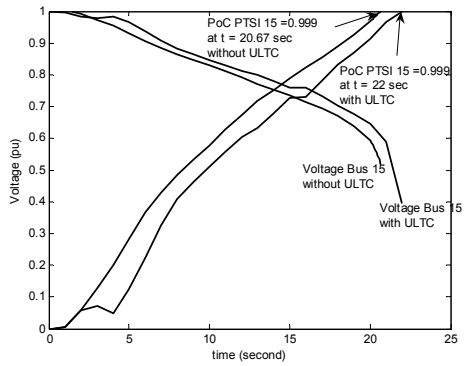

Fig. 10. PTSI index considering before and after installing ULTC

5. CONCLUSION

This paper has presented the performance of the proposed index PTSI in predicting dynamic voltage collapse. The effect of dynamic power system models such as AVR, OEL, ULTC and induction motor on voltage collapse has also been investigated. The investigation on a test system for prediction of dynamic voltage collapse, based on the PTSI index, has given encouraging results in which it is comparable to the VCPI. The proposed PTSI is a more reliable indicator for predicting because it gives the relative closeness of the stability limit. Results also prove that the PTSI give faster and more accurate voltage collapse prediction than the VCPI. From the results of the simulation, it was also observed that the increase in load reactive power has a significant impact on voltage collapse than the real power and also the system with induction motors give more effect to voltage collapse. In conclusion, it is also noted that the contingency due to load increase contributes more to voltage collapse as compared to line and generator outages.

REFERENCES

[1] Bilgari M. 2004. Dynamics of Voltage Stability in Multi Machine System, *Power system Conference and Exposition*, 1, pp. 354-359.

[2] Heydeman J., Tripathy S.C.,.Paap G.C, Sluis L. 2000. Digital and Experimental Study of Voltage Collapse and Instability in Power System, *Journal of Electrical Power and Energy System.* 22, pp. 303-311.

[3] Cai L.J and Erlich I. 2004. Dynamic Voltage Stability Analysis in Multi-Machine Power System, Retrieved December, 14, 2005, from http:// *www.uni-duisburg.de FB9/EAN/downloads/papers/ fp119.pdf*

[4] Teeuwsen. S.P., Elrich I.,El-Sharkawi M.A. 2005. Fast Eigenvalue Assessment for Large Interconnected Power Systems, *IEEE PES General Meeting*, San Franscisco.

[5] Julian D.E.,.Schultz R.P, Vu K.T. 2000. Quantance W.H., Bhatt N.B., and Novosel D., Quantifying Proximity To Voltage Collapse Using The Voltage Instability Predictor, *Proc. IEEE PES Summer Meeting*, Seatle WA, 2 , pp.931-936.

[6] Bergovic M., *Milosevic B., Novosel* D. 2002. A Novel Method for Voltage Instability Protection, *Proceeding of the 35th Hawaii International Conference on System Science.* (HICSS'02).

[7] Huang. G.M. and Nair K.L.C. 200. Detection of Dynamic Voltage Collapse. Power System Engineering Research Centre. Retrieved January 20, 2004, From the world wide web http://www.pserc.wisc.edu/ecow/get publicatio/2002 public/dynamic_summer.pdf._

[8] Balamourougan V., Sidhu T.S., Sachdev M.S. 2004. Technique For Online Prediction of Voltage Collapse, *IEE Proc-Generation, Transmission, Distribution*, 151(4) pp. 453-460.

[9] Milano F. 2006. Power System Analysis Toolbox Documentation For PSAT version Beta 1, Retrieved February 14, 2006, From : http://thunderbox.uwaterloo .ca/~fmilano.
[10] Liu Peng. 2004. Study on The Voltage Stability of Induction Motor Load, *Power System Conference and Exposition*, IEEE PES, 1 295-298.
[11] Kundur P. 1994. Power System Stability and Control, *McGraw-Hills, Inc*, New York.
[12] Silva A.S., Lerm A.A.P., Irving M. 2004 . A Basic Study of Voltage Instability with Inclusion of Limiters, *IEEE PES Transmission and distribution conference and Exposition*, pp. 548-553.
[13] Huang G., Zhang H. 2001. Detection Voltage Stability Reserve Study For Deregulated Environment, *Power System Engineering Research centre,Winter Meeting*, Retrieved Januari 20, 2005, from:http://www.pserc. wisc.edu/ecow/get/publicatio/2001public/dynamicre serve.pdf.
[14] IEEE PES. 2002. IEE PES Power System Stability subcommittee special publication on 'Voltage Stability Assessment: Concept, Practices and Tools, *Product Number SP101PSS*, Chapter 4.
[15] Haque M.H. 2003. On-line Monitoring of Maximum Permissible Loading of a Power System Within Voltage Stability Limits, *Proc.IEEE GTD*, Vol.150.No. 1, January 2003, pp107-112.
[16] Xu W., Masour Y. 1994. Voltage Stability Analysis Using Generic Dynamic Load Models, *IEEE Transaction on Power System*, 9(1), pp 479-493.
[17] Pai M.A. 1989. Energy Function Analysis for Power System Stability, *Kluwer Academic Publisher*, Norwell, M.A. pp. 222-227.

APPENDIX

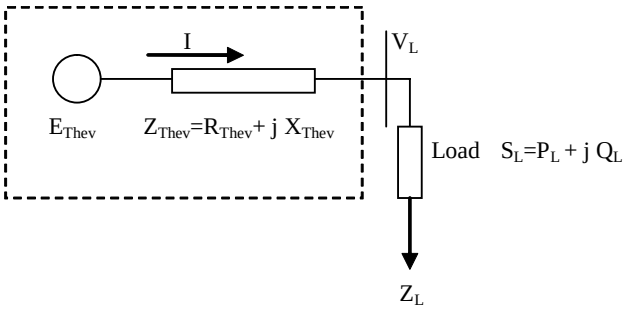

Fig. A. Simple two bus thevenin equivalen.

In order to track the Thevenin equivalent circuit, the curve fitting technique is used [6]. According to Fig. A and using the basic circuit theory:

$$\bar{E}_{Thev} = \bar{V} + \bar{I}Z_{Thev} \qquad \text{(A.1)}$$

The load bus voltage and current are measurable quantities. Hence the two unknown variables are $\bar{E}_{Thev}$ and Z_{Thev}. Decompose the vector as:

$\bar{E}_{Thev} = E_R + jE_i$, $\bar{V}_L = V_R + jV_i$ and $\bar{I} = I_R + jI_R$.

Thus, (15) can be written in matrix form as :

$$\begin{bmatrix} 1 & 0 & -I_r & I_i \\ 0 & 1 & -I_i & -I_r \end{bmatrix} \begin{bmatrix} E_r \\ E_i \\ R_{Thev} \\ X_{Thev} \end{bmatrix} = \begin{bmatrix} V_r \\ V_i \end{bmatrix} \qquad \text{(A.2)}$$

In order to solve (11), two or more measurements are required to estimate the unknown thevenin equivalent parameter.